J. Biochem. 123, 78-86 (1998)

Stability of the C-Terminal α-Helical Domain of Bacteriorhodopsin That Protrudes from the Membrane Surface, as Studied by High-Resolution Solid-State ^{13}C NMR[1]

Satoru Yamaguchi,* Satoru Tuzi,* Toshizo Seki,* Michikazu Tanio,* Richard Needleman,† Janos K. Lanyi,‡ Akira Naito,* and Hazime Saitô*,[2]

*Department of Life Science, Himeji Institute of Technology, Harima Science Garden City, Kamigori, Hyogo 678-12; †Department of Biochemistry, Wayne State University, Detroit, MI 48201, USA; and ‡Department of Physiology and Biophysics, University of California, Irvine, CA 92717, USA

Received for publication, July 25, 1997

We have recorded ^{13}C NMR spectra of [1-^{13}C]Ala- and [3-^{13}C]Ala-bacteriorhodopsin (bR), [1-^{13}C]Ala- and [3-^{13}C]Ala-papain-cleaved bR, and [3-^{13}C]Ala-labeled R227Q bR mutant by cross polarization-magic angle spinning (CP-MAS) and dipolar decoupled-magic angle spinning (DD-MAS) methods. The pH and temperature were varied, and Arg 227 was replaced with Gln (R227Q), in order to clarify their effects on the stability of the α-helical domain of the C-terminus that protrudes from the membrane surface. The comparative ^{13}C CP- and DD-MAS NMR study of [3-^{13}C]Ala-bR, rather than [1-^{13}C]Ala-bR, turned out to be the best means to distinguish the ^{13}C NMR signals of the C-terminus from those of the rest of the transmembrane helices or loops. The inner segment of the C-terminus, from Ala 228 to Ala 235, forms an α-helical domain (resonated at 15.9 ppm) either at neutral pH and/or at 10 to −10°C. The α-helical peak was not seen, however, after either cleavage of the C-terminus with papain or lowering the pH to 4.25. This α-helical structure, and a part of the random coil which was produced from the helix at pH 4.25, were further converted to a low-temperature-type α-helix, as indicated by an upfield displacement of the ^{13}C NMR signal, when the temperature was lowered to 10--10°C. Surprisingly, the corresponding helical structure in R227Q is more stable than in the wild type at the acidic pH. This α-helical peak was classified as an α_{II}-helix from the ^{13}C chemical shifts of Cβ carbon, although it was ascribed to an α_{I}-helix on the basis of the carbonyl shifts. This is in contrast to Ala 53 which adopts the α_{II}-helix as judged from the ^{13}C chemical shifts of Cβ and the carbonyl carbons. Therefore, this discrepancy might be caused by differential sensitivity of the two types of carbon signals to conformation and to modes of hydrogen bonding when motional fluctuation is involved. It is likely that the α_{II}-helix form present at the C-terminus is not always the type originally proposed but should be considered as a form undergoing large-amplitude conformational fluctuation around α-helix.

Key words: bacteriorhodopsin, ^{13}C NMR, high-resolution solid-state NMR, stability of C-terminal α-helical domain.

It is very important to gain insight into the conformation and dynamics of surface residues in membrane proteins, such as the extramembrane loops and the N- or C-termini, since part of all membrane-mediated processes occurs at the aqueous interface. These regions are difficult to characterize by means of X-ray diffraction or cryo-electron microscopy, however, because they often assume disordered conformation, and in any case the proteins do not readily form three-dimensional crystals. We have used bacteriorhodopsin (bR) from *Halobacterium salinarium* as a model integral membrane protein for examining these questions. bR is the light-driven proton pump that translocates protons from the inside to the outside of the cell (*1-4*). X-ray, neutron diffraction, and cryo-electron microscopic studies have yielded considerable structural information about the intramembrane portion of this protein (*5-11*), but little is known about the disposition of the loops, and the N- or C-terminus. The multi-dimensional NMR approach is not suitable for this purpose because of the high molecular weight of the membrane protein when surrounded by lipids or detergents.

Based on labeling of bR with different types of fluorescent probes, two different views have been presented as to the organization of the carboxyl terminus: Renthal and co-

[1] This work was supported in part by a Grant-in-Aid for Scientific Research from the Ministry of Education, Science, Sports and Culture of Japan (0645466).

[2] To whom correspondence should be addressed. Phone: +81-7915-8-0181, Fax: +81-7915-8-0182, E-mail: saito@sci.himeji-tech.ac.jp

Abbreviations: bR, bacteriorhodopsin; CP-MAS, cross polarization-magic angle spinning; DD-MAS, dipolar decoupled-magic angle spinning; NMR, nuclear magnetic resonance; T_1^C, carbon spin-lattice relaxation time; $T_1\rho^H$, proton spin-lattice relaxation time in the rotating frame; T_{CH}, cross-polarization time; R227Q, site-directed mutant protein of bR in which Arg 227 was replaced with Gln.

workers (*12*) showed that the C-terminal tail of bR is rigidly held at the membrane surface on the basis of the behavior of a hydrophobic probe, whereas Marque and coworkers (*13*) showed that the C-terminus of bR is free to assume many positions on the basis of a hydrophilic probe. There was also controversy from early ^{13}C NMR measurements as to whether the C-terminal tail freely undergoes reorientational motion or not (*14, 15*), although the latter ^{13}C NMR study using [1-^{13}C]Leu-probe was not pertinent to this problem. These fluorescence and NMR approaches were not sensitive to, or concerned with, the conformational features of the individual residues involved. On the other hand, we have recently demonstrated, based on conformation-dependent ^{13}C chemical shifts (*16–18*), that the C-terminus between residues 245 and 248, containing two Ala residues, is virtually disordered and undergoes rapid motions but the inner segment, between residues 231 and 244, with four Ala residues, participates in an ordered α-helical conformation (*19, 20*). Engelhard *et al.* (*21*) also showed that the C-terminus is fixed to the membrane *via* salt bridges between divalent cations and neighboring charges of the C-terminus as well as the interhelical loops. Nevertheless, it is not yet clear how the stability of this α-helical domain is influenced by environmental factors such as pH, temperature, metal ions, the extent of hydration, *etc.*, which are strongly related to its various kinds of interactions with amino-acid residues at the membrane surface and/or lipids.

This sort of information is important, since bR can be considered as a convenient model for better understanding of the secondary folding of surface residues for a variety of membrane proteins. We anticipated that the stability of the protruding α-helical domain would be strongly influenced by the surface pH, which controls the ionization state of side-chains (*22*), and by electrostatic interactions in the form of salt-bridges between Glu and Arg residues that are 7 residues apart in the primary peptide sequence. Accordingly, we studied the effects of cleavage by papain or replacement of Arg with an uncharged amino-acid residue such as Gln, utilizing site-directed mutant R227Q protein (*23*) as a means to modify the expected electrostatic interactions. In this connection, it was of interest to examine how conformational change of the protein backbone is induced in R227Q protein, since Arg 227 influences the rate of Schiff base reprotonation during the photocycle of bR (*23*).

Here we present further evidence for the presence of the α-helical domain protruding from the membrane surface of [3-^{13}C]Ala-labeled bR by means of high-resolution solid-state DD-MAS and CP-MAS ^{13}C NMR spectroscopy at various values of pH and temperature. This is because ^{13}C signals from the surface N- or C-terminus domains are only visible by the former technique because of the rapid tumbling motions, like those in the solution state. For this reason, a comparative study using CP-MAS and DD-MAS methods as a function of the differential rate of cross polarization dynamics is prerequisite to distinguish a protruding α-helical domain from transmembrane α-helices.

MATERIAL AND METHODS

Sample Preparation—L-[3-^{13}C]- or L-[1-^{13}C]alanine were purchased from CIL, Andover, MA, and used without further purification. *H. salinarium* strain S9 was grown in the TS medium of Onishi *et al.* (*24*), in which an unlabeled L-alanine was replaced by [3-^{13}C]L-alanine. The site-directed mutant proteins A53G and R227Q were labeled with [1-^{13}C]- and [3-^{13}C]L-alanine, respectively, in a similar manner. Purple membrane was isolated by the method of Oesterhelt and Stoeckenius (*25*) and suspended in 5 mM citrate buffer adjusted to either pH 4.25 or 6.50. Proteolysis with papain [EC 3.4.22.2] was carried out by the method of Liao and Khorana (*26*). The samples thus prepared were concentrated by centrifugation and placed into a 7.5 mm o.d. or 5 mm o.d. zirconia pencil-type rotor for magic angle spinning. The caps were tightly glued to the rotor with Rapid Araldyte to prevent leakage or evaporation of water molecules from the fully hydrated samples under the dried stream of air for magic angle spinning.

Measurements of ^{13}C NMR Spectra—High-resolution solid-state ^{13}C NMR spectra were recorded in the dark on a Chemagnetics CMX-400 NMR spectrometer, by cross polarization-magic angle spinning (CP-MAS) and dipolar decoupled-magic angle spinning (DD-MAS) with a single pulse excitation method. The spectral width, contact time, and acquisition time for CP-MAS experiments were 40 kHz, 1 ms, and 25 ms, respectively. Repetition time was 4 s for both CP-MAS and DD-MAS experiments for [3-^{13}C]-Ala-bR. DD-MAS NMR spectra for [1-^{13}C]Ala-bR were acquired with flip angles of $\pi/2$-$\pi/4$ and repetition times of 4–10 s. Free induction decays were acquired with 1K data points and Fourier-transformed as 8K data points after 7K data points were zero-filled. Carbon spin-lattice relaxation times T_1^C, as recorded by DD-MAS NMR, were measured by the standard inversion recovery method. The $\pi/2$ pulses for carbon and proton were 5–6 and 4.5–5 μs for 7.5 and 5 mm probes, respectively, and the spinning rates were 2.6–3.0 kHz. Resolution-enhancement was performed by the method of Gaussian multiplication. Transients were accumulated 2,000–8,000 times, until a reasonable signal-to-noise ratio was achieved. The ^{13}C chemical shifts were referred to the carboxyl signal of glycine (176.03 ppm from TMS) and then expressed as relative shifts from the value of tetramethylsilane (TMS).

RESULTS

Figure 1 shows the ^{13}C DD-MAS NMR spectra of [3-^{13}C]Ala-bR recorded at pH 6.5 (A) and 4.25 (B), together with their deconvoluted spectra (C and D, respectively). These well-resolved signals arose from fully hydrated bR samples in the form of pellets. The spectral resolution of a sample first lyophilized and then exposed overnight to 100% relative humidity seemed to be less good (*19, 27*). As demonstrated previously, the ^{13}C NMR signals from the region 14–18 ppm were ascribed to [3-^{13}C]Ala-bR, and the signals at 22.5 and 19.5 ppm (not shown) were assigned to the two types of methyl groups in fatty acyl chains in the lipids, to which [3-^{13}C]Ala was metabolically partially converted (*20*). It appears that the intensity of the peak at 16.8 ppm (random coil form) is significantly increased (by at least one carbon, from the deconvoluted spectra), and the intensity at 15.9 ppm [α_{II}-helix (*20, 28*); at least one carbon] is decreased at pH 4.25 compared with pH 6.5, as partially painted out with black and also indicated by the

arrows. Figure 1 also illustrates deconvoluted ^{13}C DD-MAS NMR spectra of bR both at pH 6.5 (E) and 4.25 (F) at 10°C, as compared with those at ambient temperature (20°C) (C and D). It is noteworthy that the peak-intensity at 15.6 ppm was appreciably increased at low temperature (10°C, pH 6.5) (three carbons) at the expense of part of the peak at 15.9 ppm (five carbons), as partly painted out with black. Almost the same result was obtained from the ^{13}C DD-MAS NMR spectrum recorded at −10°C at pH 7.0 (spectrum not shown). This is also true at pH 4.25 (Fig. 1, D and F). The relative proportions of this low temperature-type helix, 15.6 ppm (n_l) to the α_{II}-helix (n_a), 15.9 ppm were estimated from the deconvoluted spectra and are summarized in Table I.

In a similar manner, the intensity of the peak at 15.9 ppm under consideration was decreased, whereas the intensity at 16.8 ppm (random coil) was increased when the pH of the sample was shifted from 6.5 to 4.25, as recorded by CP-MAS NMR (Fig. 2). The observed change in the peak intensity was only about 0.6 carbon in this case, as compared with 2 carbons by DD-MAS, however. Figure 3 illustrates the ^{13}C CP-MAS (A) and DD-MAS (B: $\pi/4$ pulse with repetition time of 10 s and C: $\pi/2$ pulse with repetition time of 4 s) NMR spectra of [1-^{13}C]Ala-bR at pH 6.5. It is noteworthy that there are 11 carbonyl signals from 173.0 to 178 ppm, and only three major signals were resolved in the CP- and DD-MAS NMR spectra, respectively, reflecting their differential mobility. In addition, four carbonyl ^{13}C NMR peaks are visualized in the DD-MAS NMR spectrum of [1-^{13}C]Ala-bR arising from the loop

TABLE I. **The relative proportion of the peak-intensity of the low-temperature-type helix (n_l) to that of the α_{II}-helix (n_a) (n_l/n_a).**

	Temperature (°C)	pH 6.5[a]	pH 4.25
Wild type	−10	1.18[b]	—
	10	1.32	0.91
	20	0.22	0.38
R227Q	0	—	0.97
	10	2.10	0.83
	20	0.22	0.29

[a]5 mM citrate buffer. [b]pH 7.0 using 5 mM HEPES buffer.

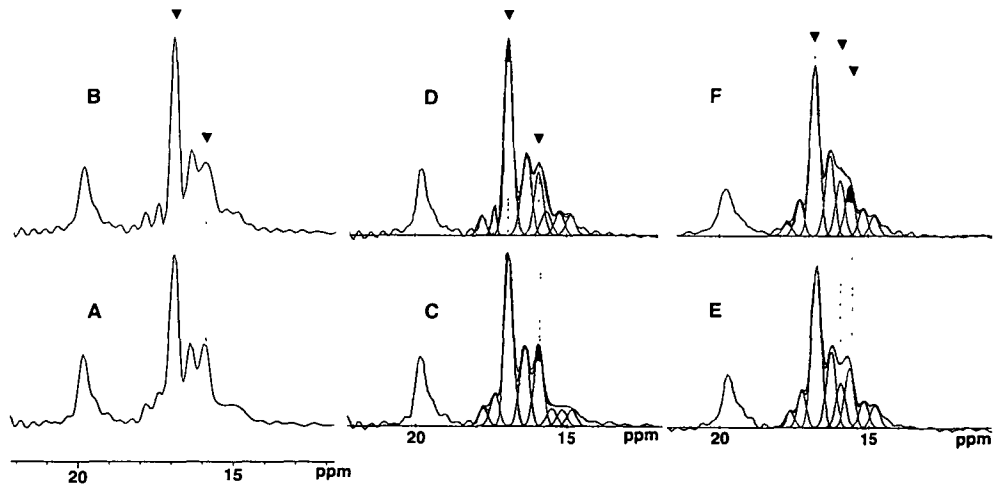

Fig. 1. **^{13}C DD-MAS NMR spectra of [3-^{13}C]Ala-bR at 20°C.** Measurements at pH 6.5 (A) and pH 4.25 (B). (C) and (D) are deconvoluted spectra of (A) and (B), respectively. The peaks whose intensity was changed are denoted by the arrows. ^{13}C DD-MAS NMR (deconvoluted) spectra of [3-^{13}C]Ala-bR at 10°C at pH 6.5 (E) and pH 4.25 (F).

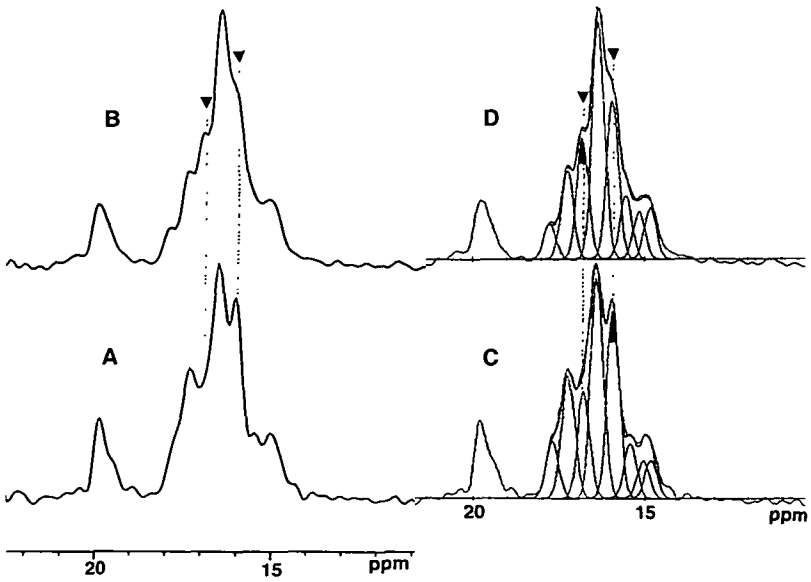

Fig. 2. **^{13}C CP-MAS NMR spectra of [3-^{13}C]-Ala-bR at 20°C.** Measurements at pH 6.5 (A) and pH 4.25 (B). (C) and (D) are deconvoluted spectra of (A) and (B), respectively.

region containing five Ala residues when the C-terminal residues have been cleaved by papain, as demonstrated in Fig. 3D. It is noteworthy that a new peak emerged at 174.4 ppm (asterisked) as a result of cleavage, and is ascribable to Ala 228 located at the newly created C-terminus of papain-treated bR. The peak positions of the remaining eight minor peaks as well as those of the three major peaks in the DD-MAS spectrum were identical with those observed in the CP-MAS within the experimental error, as summarized in Table II. In contrast to [3-^{13}C]Ala-bR, however, it is not easy to distinguish the relative contributions of the domains at the membrane surface from the transmembrane helices, because the peak intensities of the latter vary strongly with the repetition time. In order to clarify this point, we measured ^{13}C T_1[C] values of the major peaks by DD-MAS as summarized in Table II. In Fig. 3E we also included the difference of the ^{13}C CP-MAS NMR spectra of [1-^{13}C]Ala-bR for the wild type and A53G, which is unambiguously ascribable to the carbonyl peak of Ala 53 (177.9 ppm) with reference to the standard peak position of the α_{II}-helix conformation.

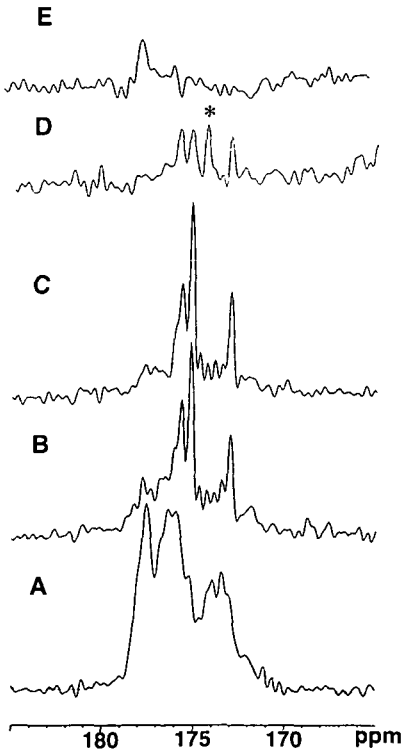

Fig. 3. **^{13}C CP-MAS NMR (A) and DD-MAS NMR (B: $\pi/4$ pulse with repetition time of 10 s, C: $\pi/2$ pulse with repetition time of 4 s) spectra of [1-^{13}C]Ala-bR at pH 6.5 and 20°C.** ^{13}C DD-MAS NMR spectrum (D) of [1-^{13}C]Ala-labeled papain-cleaved bR at 20°C (HEPES buffer, pH 7; $\pi/2$ pulse with repetition time of 4 s). The asterisked peak arose from a newly created looped structure due to cleavage by papain. The difference CP-MAS NMR spectrum (E) between [1-^{13}C]Ala-labeled wild type and A53G is also given.

Figure 4 illustrates the ^{13}C DD-MAS NMR spectra of papain-treated [3-^{13}C]Ala-bR, together with the corresponding deconvoluted spectra, both at pH 6.5 (A and C) and 4.25 (B and D), in order to clarify whether the above-mentioned peak change really originates from the C-terminal residues protruding from the surface. Papain cleaves between Glu 232 and Gly 231. No spectral change as found in Fig. 1 is seen in this case, because the residues responsible had been removed. Nevertheless, it is interesting to note that the major spectral change owing to the cleavage is the displacement of at least one carbon signal from the α_{II}-helix at 16.9 ppm to the loop region at 17.3 ppm, as partly painted out with black and shown by the arrows in the DD-MAS NMR spectrum (see Fig. 4, A and C, as compared with Fig. 1, A and C). There is no peak-intensity change at 15.9 ppm for the papain cleaved preparation with pH change. This superimposed peak (17.3 ppm) at pH 6.5 (Fig. 4, A and C), however, was further displaced upfield by 0.4 ppm to the peak at 16.9 ppm, at pH 4.25 (Fig. 4, B and D). A similar result was obtained in the CP-MAS NMR spectra, although the intensity change at 17.3 ppm (painted with black) is less pronounced than that in the DD-MAS spectrum (Fig. 5). It should be noted that the newly created loop peak (17.3 ppm) due to the cleavage by papain in Fig. 4C also gives rise to the new peak at 174.4 ppm (asterisked) for the papain-cleaved preparation (Fig. 3D).

Figure 6 shows the CP-MAS NMR spectrum of the R227Q protein at pH 6.5 (A), as compared with the wild type (B) and the DD-MAS NMR spectra of R227Q at pH 4.25 and 10°C (C) and 20°C (D). The peak indicated by the arrow (16.9 ppm) is enhanced in R227Q (Fig. 6A) by the amount of 0.4 carbon, at the expense of the peak at 17.3 ppm as compared with those of the wild type (Fig. 6B). No change, however, was observed in the DD-MAS NMR spectra (spectra not shown). In this sample we examined how the secondary structure at the cytoplasmic surface of this protein and the helical structure are modified by

TABLE II. **^{13}C chemical shifts and spin lattice relaxation times of [1-^{13}C]Ala-bR (ppm from TMS).**

Conformation	bR			Papain-treated	Reference data	
	CP-MAS	DD-MAS	T_1(s)	DD-MAS	α_I-helix[a]	α_{II}-helix[b]
Loop	173.0	173.0	1.43	173.0	—	—
	173.4	(173.4)[c]	—	—	—	—
	173.9	(173.8)[c]	—	—	—	—
	174.3	(174.2)[c]	—	174.4	—	—
	174.7	(174.7)[c]	—	—	—	—
Random coil	175.2	175.2	1.36	175.3	—	—
α-helix	175.9	175.7	1.76	175.8	—	—
	176.3	(176.2)[c]	—	—	176.4	—
	176.7	(176.8)[c]	—	—	—	—
	177.5	(177.3)[c]	—	—	—	—
	178.0	(177.7)[c]	—	—	—	177.9

[a]C=O ^{13}C chemical shifts form solid $(Ala)_n$. [b]Difference spectrum between [1-^{13}C]Ala-labeled wild and A53G. [c]Minor component.

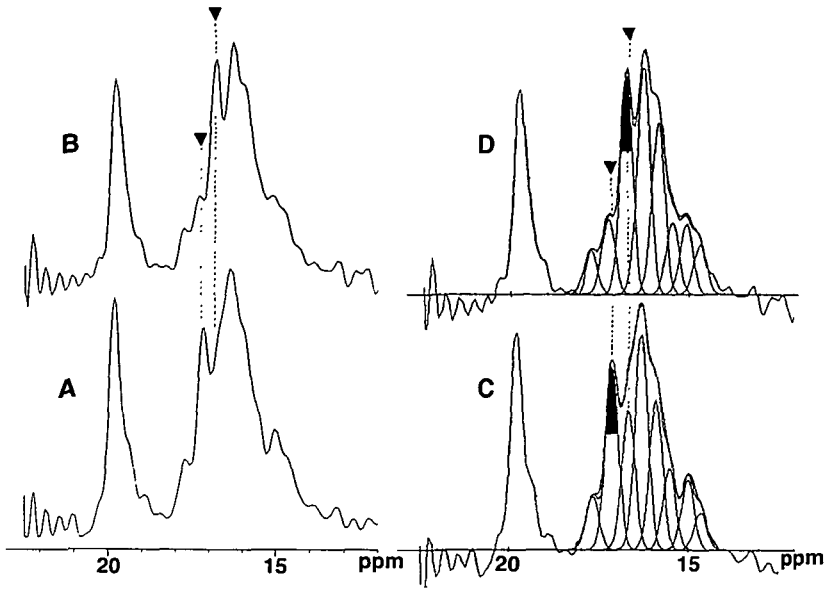

Fig. 4. **^{13}C DD-MAS NMR spectra of [3-^{13}C]-Ala-labeled papain-cleaved bR at 20°C.** Measurements at pH 6.5 (A) and pH 4.25 (B). (C) and (D) are deconvoluted spectra of (A) and (B), respectively.

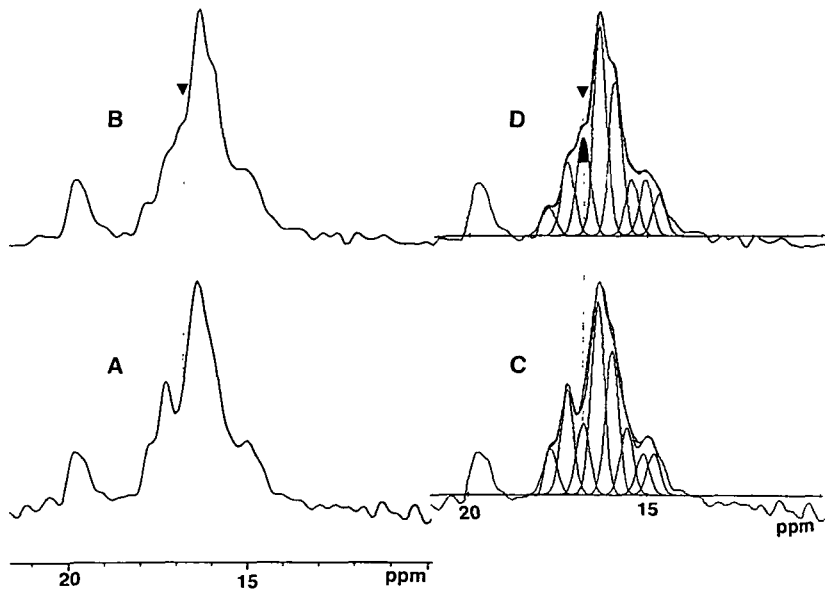

Fig. 5. **^{13}C CP-MAS NMR spectra of [3-^{13}C]-Ala-labeled papain-cleaved bR at pH 6.5 (A) and pH 4.25 (B) at 20°C.** (C and D are deconvoluted spectra of A and B, respectively).

replacement of one of the Arg residues in the vicinity of the C-terminus with Gln. The α_{II}-helix peak (15.9 ppm) of R227Q protein was not disrupted even at pH 4.25 (Fig. 6D), but it was converted to the low temperature-type helix (15.6 ppm) at 10°C in a similar manner to that of the wild type (Fig. 6C). The peak intensity of the low temperature helix at 15.6 ppm in the R227Q protein was further increased at 0°C, instead of a further upfield displacement. The n_l/n_a values for R227Q protein are also summarized in Table I.

DISCUSSION

Conformation-Dependent Assignments of Peaks: [3-^{13}C]-Ala Signals—In order to relate the ^{13}C NMR spectral changes to protein conformation, it is essential to be able to assign all the observed ^{13}C NMR peaks. We have attempted to assign the observed ^{13}C NMR peaks of [3-^{13}C]Ala-bR to individual Ala residues with reference to (i) the accumulated data of the conformation-dependent displacements of ^{13}C chemical shifts (*16-18*), (ii) difference spectra between intact and enzymatically digested bR (*19*), (iii) difference spectra between wild and mutant strains of [3-^{13}C]Ala-bR (*20*), and (iv) chemically synthesized and selectively [3-^{13}C]Ala-labeled fragments of bR incorporated into lipid bilayers (*29*). We have so far completed assignment of all the signals from the C- and N-termini on the basis of the aforementioned steps (i) and (ii), although the peak assignment to the transmembrane helices and loops has not yet been finished. In particular, the peak at 16.9 ppm was assigned to Ala 245-248 at the terminal end (see Fig. 4 for the difference spectra between intact and enzymatically cleaved preparation) using the conformation-dependent displacement of peaks (*19, 27*). Here, we assigned part of

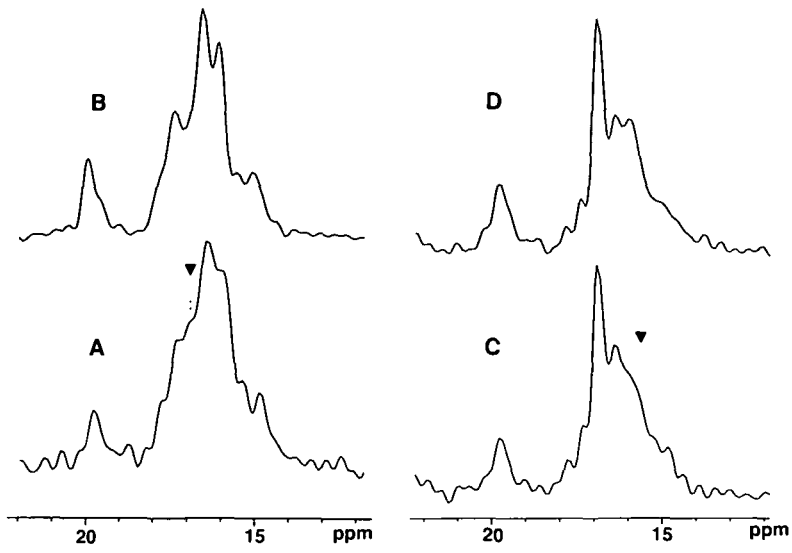

Fig. 6. ^{13}C CP-MAS NMR of [3-^{13}C]Ala-labeled R227Q protein (A) as compared with that of wild type (B) at pH 6.5 at 20°C, DD-MAS NMR spectrum of R227Q at pH 4.25 and 10°C (C) and at 20°C (D).

the peak (at least one carbon) at 15.9 ppm to Ala residues (228 and 233) by taking into account their peak intensities in the intact [five carbons from the deconvoluted spectrum for a total of 29 Ala residues (Fig. 1C)] and papain cleaved (three carbons) bRs. It is likely that the ^{13}C NMR peak of Ala 235 appears at 16.9 ppm in spite of its position in the C-terminus helix, considering that six Ala residues (Ala 2, 235, 240, 244, 245, and 246) should take the random coil configuration at the membrane surface from the differential peak intensities between the DD-MAS (11 carbons) and CP-MAS (3 carbons) NMR of intact bR. Besides, we found that Ala 103 is also in the random coil form, based on our recent ^{13}C NMR study on [3-^{13}C]Ala-labeled A103C protein (unpublished). This is understandable because this Ala 235 is in the neighborhood of Pro 238 at the terminal position of the α-helix, and is likely to be partially mobilized. In fact, Pro 238 was proposed to be in a position where the tail becomes freely mobile (*21*).

It is interesting to note that the one carbon signal at 15.9 ppm disappeared in the DD-MAS NMR spectrum after papain cleavage at Gly 231 (compare Figs. 1 and 4). The peak intensity of the loop region at 17.3 ppm increased (by one carbon) at pH 6.5, as a result of forming a looped structure instead of an α-helical domain containing Ala 228. This looped structure, however, was disrupted at pH 4.25 (Fig. 4B), resulting in conversion to random coil. It is possible that the looped structure is formed by anchoring to the surface through ionic interaction between the negative charge at the newly created C-terminus GlyO- and the positively charged side-chains of amino acid residues. At a pH of 4.25, GlyO- would be normally charged in the bulk solution, but it might be protonated at the much lower surface pH. Therefore, this looped structure would be destabilized and converted to a random coil.

[1-^{13}C]Ala Signals—The carbonyl ^{13}C NMR peaks are well resolved to 11 peaks (Fig. 3A) which could be assigned with reference to the ^{13}C chemical shifts of the α_I-helix and β-sheet forms, 176.4 and 171.8 ppm, respectively (*16, 17*). In addition, the most intense peak at 175.2 ppm in the DD-MAS NMR spectrum (Fig. 3B) is straightforwardly assigned to the C-terminal end Ala residues that assume the random coiled form, in view of its peak position (*30*) as well as a shortened spin-lattice relaxation time (1.36 s) due to the acquisition of rapid reorientational motion (Table II) as a result of taking random coil conformation. However, the same peak visible in the CP-MAS NMR spectrum can not necessarily be ascribed to this type of random coil form in view of its anisotropic environment as detected by CP-MAS NMR as discussed before in relation to the ^{13}C NMR signals from [3-^{13}C]Ala-bR (16.9 ppm) (*19, 20*). Therefore, it is more probable that this signal is ascribed to Ala residues, located near the surface of the membrane, taking the transmembrane α-helices but undergoing thermal fluctuation involving fraying of the transmembrane helices. In this connection, it is interesting to note that the corresponding peak at 16.9 ppm is displaced upfield to assume the α_{II}-helix form when Schiff base was removed either by solubilization with SDS (Tanio *et al.*, manuscript in preparation) or bleaching to yield bacterioopsin (*20*). It is therefore expected that the five peaks of the CP-MAS NMR spectrum in the region lower than 175.9 ppm are ascribed to α-helix form, although these peaks could be displaced further from the standard value if distorted α_{II}-helices are present (*31*), as already demonstrated from the [3-^{13}C]Ala signals. In fact, the carbonyl ^{13}C NMR peak of Ala 53 turned out to lie at 177.9 ppm on the basis of the difference spectrum between wild and A53G proteins (Fig. 3E). This means that the [3-^{13}C]- (16.3 ppm) and [1-^{13}C]- (177.9 ppm) Ala 53 peaks are both very close to the reference values for α_{II}-helix (15.8 and 178.4 ppm, respectively) as observed for $(Ala)_n$ in HFIP solution (*19*).

The second intense peak at 175.6 ppm in the DD-MAS NMR spectrum (Fig. 3B) was straightforwardly ascribed to the α-helical domain under consideration at the C-terminus, because its peak intensity was reduced by 50% in the papain-cleaved protein (Fig. 3D), and its intensity varied when the flip-angle and repetition time were changed (Fig. 3C). It is difficult to understand why this peak position or the intensity do not vary significantly with pH or temperature as mentioned above, as in the case of [3-^{13}C]Ala-bR. It is surprising that the carbonyl ^{13}C NMR peak for this α-helix (175.6 ppm) is far from the reference value for the

α_{II}-helix (177.9 ppm), although the α_{II}-helix is evident from the Cβ signals. This is in contrast to the assignment of Ala 53 located at the transmembrane α-helix which takes the α_{II}-helix form as judged from the ^{13}C chemical shifts of Cβ and the carbonyl carbons. This situation could be modified when molecular motions are present, because the Cβ ^{13}C chemical shifts are mainly influenced by the conformation as defined by the torsion angles, while the carbonyl ^{13}C chemical shifts are influenced by both the conformation as defined by the torsion angles and the modes of hydrogen bonding (*17*). Then, differential responsiveness to these factors might result in such an apparent discrepancy in the prediction of the conformations involved. The remaining two signals, at 173.0 and 174.4 ppm, in the DD-MAS NMR spectrum of papain cleaved bR could be ascribed to Ala residues at the surface which acquire motional freedom as loops. In particular, the Ala 228 signal is ascribed to the peak at 174.4 ppm which is ascribed to a newly created loop, consistent with the signal of [3-^{13}C]Ala-bR at 17.3 ppm after cleavage by papain (Fig. 4C). In a similar manner, the five signals between 173.0 and 174.7 ppm were resolved in the CP-MAS NMR spectrum owing to their reduced motional freedom, even if they lie in a loop region at the membrane surface. Further experiments are necessary for peak assignment, however.

Dynamics of the C-Terminus Helix—As pointed out already, two [3-^{13}C]Ala carbon signals of DD-MAS NMR spectra were assigned to the α-helical domain formed at pH 6.5 (Fig. 1), whereas only 0.6 carbon in the CP-MAS NMR (Fig. 2) was assigned to this region. It is likely that this difference arises mainly from a differential responsiveness to the conformational change that occurs in regions where rapid or intermediate molecular motions are present. The peak intensities of the DD-MAS NMR spectra are correctly acquired for all portions only when the following condition is satisfied,

$$t > 5\ T_1^C \qquad (1)$$

where t and T_1^C are the repetition time and carbon spin-lattice relaxation time, respectively. This condition is easily satisfied when DD-MAS NMR spectra are recorded for [3-^{13}C]Ala-bR with the repetition time of 4 s and carbon spin-lattice relaxation time of 0.5 s (*27*). In contrast, the ^{13}C NMR peak-intensities recorded by CP-MAS NMR are not always proportional to the carbon numbers unless the following condition is satisfied:

$$T_{1\rho}^H > \text{contact time} > T_{CH}, \qquad (2)$$

where $T_{1\rho}^H$ and T_{CH} are proton spin-lattice relaxation times in the rotating frame and cross polarization time, respectively. The cross polarization time T_{CH} for bR is about 100–200 μs (*20*), but is expected to be appreciably prolonged for regions such as the C-terminal tail in which dipolar interactions are almost time-averaged, as in the lipid methyl signals of purple membrane (longer than 10 ms). The $T_{1\rho}^H$ values for the transmembrane helices and loops are approximately 5–7 ms (*20*). Therefore, signals from the C-terminus might be partly or fully suppressed by choosing conditions to obtain the maximum peak intensities from the transmembrane portions utilizing the contact time of about 1 ms. This is exactly the case for the ^{13}C CP-MAS NMR spectra of [3-^{13}C]Ala-bR in which almost all the ^{13}C signals from the mobile portions are partially or completely suppressed, depending upon their respective correlation times.

The condition allowing observation of the whole spectra in DD-MAS is very stringent for [1-^{13}C]Ala, because the T_1^C value for carbons at the transmembrane helices are of the order of 10–20 s (unpublished). Obviously, recording of ^{13}C signals from regions in which both T_1^C and T_{CH} values are longer by both CP- and DD-MAS NMR measurements is not easy, although several peaks for the latter could be recorded by using a longer repetition time (10 s) and a small flip angle ($\pi/4$ pulse). This is the reason why only four ^{13}C signals from [1-^{13}C]Ala were visible in the DD-MAS experiment, in contrast to the case of [3-^{13}C]Ala-labeling. Thus, DD-MAS is not always suitable for locating the protruding α-helical region from carbonyl signals.

It appears that the protruding α-helix under consideration is not always as rigid as might be expected from its ordered structure, but undergoes reorientational motions with correlation times of the order of 10^{-8} s, as judged from the fact that the signals from this region are only partially (0.6 carbon in spite of two carbons present) visible in the CP-MAS spectra. This is presumably caused by prolonged T_{CH} values, longer than the contact time used. This timescale is consistent with the previous fluorescent probe study in which no rapid motion in the labeled tail occurred over two excited-state life times of 13–25 ns (*12*). It should be emphasized that this helical region is not stabilized when the C-terminus is removed from the membrane surface (*27*). It is also likely that this region could be considered as disordered from a crystallographical point of view, even though its motions were frozen at the lower temperature and could not be located by a cryo-electron microscopic study (*7, 11*).

We found that when the C-terminus was cleaved at Gly 231 the ^{13}C NMR signal of Ala 228 at pH 6.5 was not involved in an α-helix form but appeared as part of the loop region, owing to some sort of interaction with residues at the surface (Fig. 4). This is probably because six residues constitute too short a segment to be stabilized as an independent α-helix (Fig. 7), as distinguished from the transmembrane helices within the bilayer, and because one of two salt-bridges between Glu and Arg is removed, as will be discussed later. It is also interesting to note that the Ala 228 signal taking random coil conformation at pH 4.25 is still visible in the DD-MAS NMR (Fig. 4).

The Effect of Amino-Acid Substitution on Stability of the α-Helical Domain—We found that the relative proportion of the low-temperature-type helix was substantially increased at lower temperature, 10 to -10°C (Table II), in spite of the differences in the pH employed. It is emphasized that the peak position of this low-temperature-type helix (15.6 ppm) is very close to that of standard α_I-helix (14.9 ppm) (*16–18*), This means that either the torsion angle is at the normal position of α-helix or thermal fluctuation is substantially reduced. In fact, partial freezing of thermal fluctuation is a very important factor for the stabilization of the α_{II}-helix or the low-temperature-type helix that protrudes from the membrane surface. This α-helical domain might be stabilized by some sort of electrostatic interaction between side-chains. In fact, the amino acid sequence shows that there are two Arg-Glu pairs in this region in which the residues are 7 residues apart, namely Arg 227 and Glu 234, and Arg 225 and Glu 232.

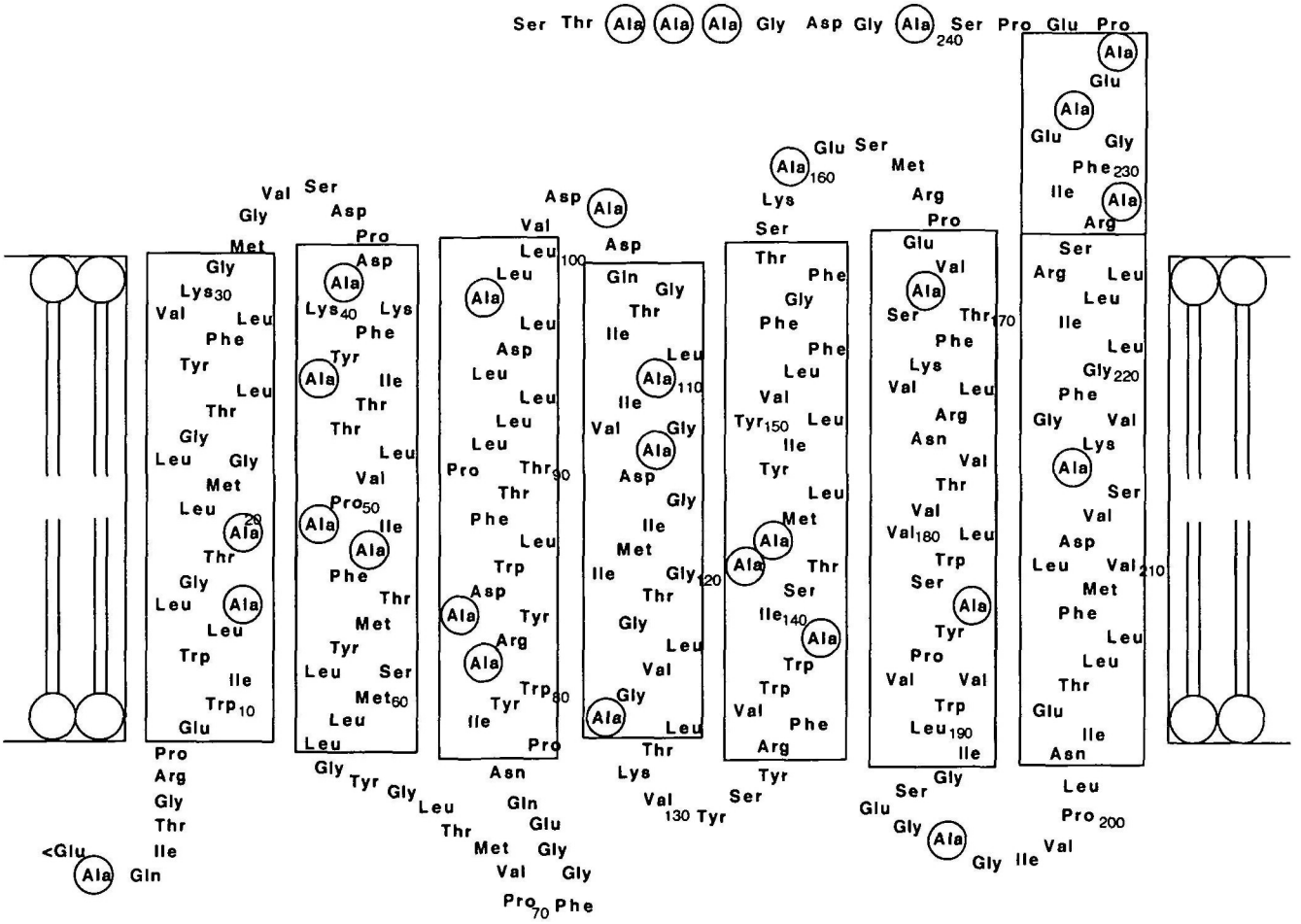

Fig. 7. **The location of the α-helix at the C-terminus as shown in the box protruding from the membrane surface** (after Ref. *11*). Ala residues are shown by circles.

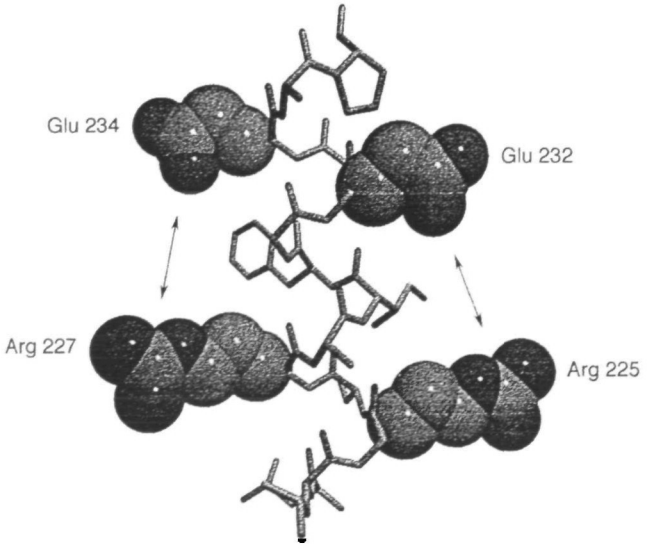

Fig. 8. **Plausible electrostatic interactions between Arg and Glu residues, responsible for the stabilization of the protruding α-helix.**

Modeling suggests that if the side-chains are in extended conformation in these pairs the positive and negative charges point in the same direction and are separated by 10 Å (Fig. 8). It was our intent partially to neutralize one of the ionic residues of these pairs by lowering the pH to 4.25, which might be close to the pK_a of Glu residues in bR. As can be seen from Figs. 1 and 2, the α-helix under consideration was indeed disrupted, consistent with our expectation. It is interesting that this disrupted helix at pH 4.25 recovered to form a low-temperature-type α-helix, when the temperature was lowered to 10°C.

The other way to alter the relative stability of this helix was to use a mutant protein, such as R227Q in which Arg 227 is replaced with the uncharged Gln. We found that the spectral change of the CP-MAS NMR spectra between the wild type and the R227Q protein is rather small, except for the peak at 16.9 ppm (which is ascribed to random coil form, but not necessarily the true "random coil" for the three or four carbons at either the transmembrane helices or loops) as mentioned above, and its intensity in R227Q is greater (as indicated by the arrow in Fig. 6A). It is interesting that the α_{II}-helix peak of the R227Q protein resonated at 15.9 ppm and was stable even at pH 4.25 and 20°C, in contrast to the case of the wild type (compare Fig. 8D with Fig. 1B). It should also be pointed out that the manner of

the conversion to the alternative helix is exactly the same as that of the wild type (see Figs. 8C and 7C). It appears, therefore, that the ionic interaction between Arg 225 and Glu 232 is more important than that between Arg 227 and Glu 234.

Concluding Remarks—The NMR approach reported here, which utilizes the quantitative comparison of peak intensities of CP-MAS with those of DD-MAS NMR of [3-^{13}C]Ala-bR, has proven to be suitable for distinguishing residues located at the membrane surface. In particular, we were able to locate a C-terminus α-helical domain protruding from the membrane surface. The NMR method therefore seems likely to be a valuable tool in studies of the conformation and dynamics of the surface region of membrane proteins in general.

REFERENCES

1. Ovchinnikov, Y.A. (1982) Rhodopsin and bacteriorhodopsin: structure-function relationships. *FEBS Lett.* **148**, 179-191
2. Stoeckenius, W. and Bogomolni, R.A. (1982) Bacteriorhodopsin and related pigments of halobacteria. *Annu. Rev. Biochem.* **52**, 587-616
3. Mathies, R.A., Lin, S.W., Ames, J.B., and Pollard, W.T. (1991) From femtoseconds to biology: Mechanism of bacteriorhodopsin's light-driven proton pump. *Annu. Rev. Biophys. Biophys. Chem.* **20**, 491-518
4. Lanyi, J.K. (1993) Proton translocation mechanism and energetics in the light-driven pump bacteriorhodopsin. *Biochim. Biophys. Acta* **1183**, 241-246
5. Wallace, B.A. and Henderson, R. (1982) Location of the carboxyl terminus of bacteriorhodopsin in purple membrane. *Biophys. J.* **39**, 233-239
6. Popot, J.L., Engelman, D.M., Gurel, O., and Zaccai, G. (1989) Tertiary structure of bacteriorhodopsin: Positions and orientations of helices A and B in the structural map determined by neutron diffraction. *J. Mol. Biol.* **210**, 829-847
7. Henderson, R., Baldwin, J.M., Ceska, T.A., Zemlin, F., Beckmann, E., and Downing, K. H. (1990) Model for the structure of bacteriorhodopsin based on high-resolution electron cryo-microscopy. *J. Mol. Biol.* **213**, 899-929
8. Koch, M.H.J., Dencher, N.A., Oesterhelt, D., Plohn, H.-J., Rapp, G., and Buldt, G. (1991) Time-resolved X-ray diffraction study of structural changes associated with the photocycle of bacteriorhodopsin. *EMBO J.* **10**, 521-526
9. Subramaniam, S., Gerstein, M., Oesterhelt, D., and Henderson, R. (1993) Electron diffraction analysis of structural changes in the photocycle of bacteriorhodopsin. *EMBO J.* **12**, 1-8
10. Schertler, G.F.X., Bartunik, H.D., Michel, H., and Oesterhelt, D. (1993) Orthorhombic crystal form of bacteriorhodopsin nucleated on benzamidine diffraction to 3.6 Å resolution. *J. Mol. Biol.* **234**, 156-164
11. Grigorieff, N., Ceska, T.A., Downing, K.H., Baldwin, J.M., and Henderson, R.H. (1996) Electron-crystallographic refinement of the structure of bacteriorhodopsin. *J. Mol. Biol.* **259**, 393-421
12. Renthal, R., Dawson, N., Tuley, J., and Horowitz, P. (1983) Constraints on the flexibility of bacteriorhodopsin's carboxyl-terminal tail at the purple membrane surface. *Biochemistry* **22**, 5-12
13. Marque, J., Kinoshita, K. Jr., Govindjee, R., Ikegami, A., Ebrey, T.G., and Otomo, J. (1986) Environmental modulation of C-terminus dynamic structure in bacteriorhodopsin. *Biochemistry* **25**, 5555-5559
14. Bowers, J.L. and Oldfield, E. (1988) Quantitative carbon-13 nuclear magnetic resonance spectroscopic study of mobile residues in bacteriorhodopsin. *Biochemistry* **27**, 5156-5161
15. Lewis, B.A., Harbison, G.S., Herzfeld, J., and Griffin, R.G. (1985) NMR structural analysis of a membrane protein: bacteriorhodopsin peptide backbone orientation and motion. *Biochemistry* **24**, 4671-4679
16. Saitô, H. (1986) Conformation-dependent ^{13}C chemical shifts: A new means of conformational characterization as obtained by high-resolution solid-state ^{13}C NMR. *Magn. Reson. Chem.* **24**, 835-852
17. Saitô, H. and Ando, I. (1989) High-resolution solid-state NMR studies of synthetic and biological macromolecules. *Annu. Rep. NMR Spectrosc.* **21**, 209-290
18. Saitô, H., Tuzi, S., and Naito, A. (1998) Empirical vs. non-empirical evaluation of secondary structure of fibrous and membrane proteins by solid-state NMR spectroscopy: a practical approach. *Annu. Rep. NMR Spectrosc.* **36**, in press
19. Tuzi, S., Naito, A., and Saitô, H. (1994) ^{13}C NMR study on conformation and dynamics of the transmembrane α-helices, loop, and C-terminus of [3-^{13}C]Ala-labeled bacteriorhodopsin. *Biochemistry* **33**, 15046-15052
20. Tuzi, S., Yamaguchi, S., Naito, A., Needleman, R., Lanyi, J.K., and Saitô, H. (1996) Conformation and dynamics of [3-^{13}C]Ala-labeled bacteriorhodopsin and bacterioopsin, induced by interaction with retinal and its analogs, as studied by ^{13}C nuclear magnetic resonance. *Biochemistry* **35**, 7520-7527
21. Engelhard, M., Finkler, S., Metz, G., and Siebert, F. (1996) Solid-state ^{13}C NMR of [(3-^{13}C)Pro]bacteriorhodopsin and [(4-^{13}C)Pro]bacteriorhodopsin. Evidence for a flexible segment of the C-terminal tail. *Eur. J. Biochem.* **235**, 526-533
22. Alexiev, U., Marti, T., Heyn, M.P., Khorana, H.G., and Scherrer, P. (1994) Surface charge of bacteriorhodopsin detected with covalently bound pH indicators at selected extracellular and cytoplasmic sites. *Biochemistry* **33**, 298-306
23. Brown, L.S., Yamazaki, Y., Maeda, A., Sun, L., Needleman, R., and Lanyi, J.K. (1994) The proton transfers in the cytoplasmic domain of bacteriorhodopsin are facilitated by a cluster of interacting residues. *J. Mol. Biol.* **239**, 401-414
24. Onishi, H., McCance, E.M., and Gibbons, N.E. (1965) A synthetic medium for extremely halophilic bacteria. *Can. J. Microbiol.* **11**, 365-373
25. Oesterhelt, D. and Stoeckenius, W. (1973) Functions of a new photoreceptor membrane. *Proc. Natl. Acad. Sci. USA* **70**, 2853-2857
26. Liao, M.J. and Khorana, H.G. (1984) Removal of the carboxyl-terminal peptide does not affect refolding or function of bacteriorhodopsin as a light-dependent proton pump. *J. Biol. Chem.* **259**, 4194-4199
27. Tuzi, S., Naito, A., and Saitô, H. (1993) A high-resolution solid-state ^{13}C-NMR study on [1-^{13}C]Ala and [1-^{13}C]Leu and Val-labelled bacteriorhodopsin. *Eur. J. Biochem.* **218**, 837-844
28. Tuzi, S., Naito, A., and Saitô, H. (1996) Temperature-dependent conformational change of bacteriorhodopsin as studied by solid-state ^{13}C NMR. *Eur. J. Biochem.* **239**, 294-301
29. Naito, A., Kimura, S., Tuzi, S., and Saitô, H. (1997) Synthesis of [3-^{13}C]Ala-labeled helix fragments of bacteriorhodopsin and their incorporation into lipid bilayers in *Peptide Chemistry 1996* (Kitada, C., ed.)pp. 369-372, Protein Research Foundation, Osaka
30. Howarth O.W. and Lilley, D.M. (1978) Carbon-13 NMR of peptides and proteins. *Prog. NMR Spectrosc.* **12**, 1-40
31. Krimm, S. and Dwivedi, A.M. (1982) Infrared spectrum of the purple membrane: clue to proton conduction mechanism? *Science* **216**, 407-408